32nd URSI GASS, Montreal, 19–26 August 2017

Complex Source Diffraction by a Cone: Exact and Asymptotic Solutions

M. Katsav[(1)], E. Heyman*[(1)], and L. Klinkenbusch [(2)]
(1) School of Electrical Engineering, Tel Aviv University, Tel Aviv, Israel
(2) Institute of Electrical and Information Engineering, Kiel University, Kiel, Germany

Abstract

The exact and asymptotic solutions to the scattering of a complex-source beam (CSB) by an acoustically soft or hard semi-infinite circular cone are explored. The exact solution, expressed as a spherical-harmonics expansion, is compared with the complex geometrical optics (CGO) solution augmented by a complex ray diffraction at the tip.

1 Introduction

The complex-source beam (CSB) provides a canonical setting for a rigorous study of various beam diffraction phenomena [1]. In the present work we explore the scattering of CSB by a semi-infinite soft or hard cone. This canonical problem contains wealth of local scattering phenomena which depend on the direction and collimation of the incident beam as well as its displacement from the tip.

Exact spherical-harmonics solution has been derived by us in the past, for both acoustic and electromagnetic waves [2]. Here we derive a complex geometrical optics (CGO) solution which is augmented by a complex ray diffraction at the tip.

2 The Incident Beam Field

We consider the scattering of a CSB by a circular PEC cone with apex angle Θ located symmetrically around the negative z-axis. The beam is collimated such that $kb \gg 1$ where b is the collimation length and $k = \omega/c$ is the wavenumber. Its direction is described by the unit vector $\hat{\mathbf{b}}$ and its waist is centered at $\mathbf{r}_0$. We are specifically interested in the case depicted in Fig. 1 where the beam hits near the tip, so that $\hat{\mathbf{b}}$ and $\mathbf{r}_0$ are defined accordingly.

In the CS approach, the incident beam wave is modeled as radiation from a source located at the complex coordinate point [3, 5]

$$\mathbf{r}_c = \mathbf{r}_0 + i\mathbf{b}, \qquad \mathbf{b} = b\hat{\mathbf{b}}, \tag{1}$$

where, for later use, we express these vectors conveniently both in Cartesian and in spherical coordinates viz $\mathbf{r}_0 = (x_0, y_0, z_0) = (r_0, \theta_0, \phi_0)$, $\mathbf{b} = (x_b, y_b, z_b) = (b, \theta_b, \phi_b)$, and we also note that if the beam hits near the tip then $\theta_0 \simeq \pi - \theta_b$, $\phi_0 \simeq \pi + \phi_0$.

In free space, the field due to the source (1) is expressed as

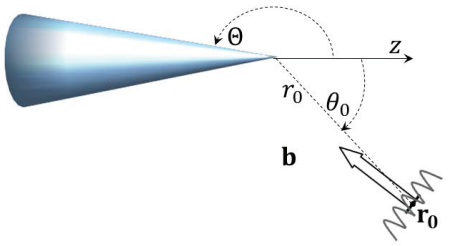

Figure 1. Beam scattering by a circular cone.

an analytic continuation of the free-space Green's function

$$G^i(\mathbf{r}, \mathbf{r}_c) = \frac{e^{iks}}{4\pi s}, \quad s = \sqrt{(x-x_c)^2 + (y-y_c)^2 + (z-z_c)^2}, \tag{2}$$

with $\mathrm{Re}\, s > 0$. s is the complex distance from $\mathbf{r}_c$ to the real observation point $\mathbf{r}$. The properties of the solution in (2) depend on the branch of the square root in s. The choice $\mathrm{Re}\, s > 0$ for all real $\mathbf{r}$ implies a brunch cut at the beam waist, centered at $\mathbf{r}_0$ (wiggly line in Fig. 1). It is referred to as the "source disk" as it represents the distribution of the physical sources in real space. The resulting field is strictly causal in the sense that it is outgoing with respect to the source disk. In the wll collimation case $kb \gg 1$, this field behaves like a Gaussian beam (GB) emerging in the $\hat{\mathbf{b}}$ direction, being weak in all other directions.

3 Exact Solution for the Scattered Field

In the presence of the cone, the field due to the source (1) can be expressed as an eigenfunction expansion [2, 3, 4]

$$G(\mathbf{r}, \mathbf{r}_c) = \frac{ik}{2\pi} \sum_{\ell=0}^{\infty} \varepsilon_\ell \cos \ell(\phi - \phi_c) \sum_{\nu>0} (2\nu+1) I_\nu^\ell \times j_\nu(kr_<) h_\nu^{(1)}(kr_>) \mathrm{P}_\nu^\ell(\cos\theta) \mathrm{P}_\nu^\ell(\cos\theta_c), \tag{3}$$

where we assume a soft boundary, j_ν and $h_\nu^{(1)}$ are spherical Bessel functions, P_ν^ℓ are the associated Legendre functions, $(r_<, r_>) = (r, r_c)$ if $r < \mathrm{Re}\, r_c$ and (r_c, r) if $r > \mathrm{Re}\, r_c$, $\varepsilon_\ell = 1$ for $\ell = 0$ and 2 otherwise, and I_ν^ℓ are normalization constants defined by

$$I_\nu^\ell = \left\{ \int_0^\Theta [\mathrm{P}_\nu^\ell(\cos\theta)]^2 \sin\theta d\theta \right\}^{-1}. \tag{4}$$

Alternatively, the solution can be expressed by the θ-

domain spectral integral [3, 6]

$$G(\mathbf{r},\mathbf{r}_c) = \frac{k}{4\pi^2}\sum_{\ell=0}^{\infty}\varepsilon_\ell \cos\ell(\phi-\phi_c)\times \int_{\mathscr{C}} d\nu\,(2\nu+1)\,j_\nu(kr_<)h_\nu^{(1)}(kr_>)g_\theta, \quad (5)$$

where g_θ, the θ-domain 1D Green's function, is a sum of the free-space and scattered Green's functions

$$\left.\begin{matrix} g_\theta^i(\theta,\theta_c) \\ g_\theta^s(\theta,\theta_c) \end{matrix}\right\} = -\frac{\pi}{2}\frac{\Gamma(\nu+\ell+1)\mathrm{P}_\nu^{-\ell}(\cos\theta_<)}{\Gamma(\nu-\ell+1)\sin(\nu-\ell)\pi} \times \begin{cases} \mathrm{P}_\nu^{-\ell}(-\cos\theta_>) \\ -\frac{\mathrm{P}_\nu^{\ell}(-\cos\Theta)}{\mathrm{P}_\nu^{\ell}(\cos\Theta)}\mathrm{P}_\nu^{\ell}(\cos\theta_>), \end{cases} \quad (6)$$

with $(\theta_<,\theta_>) = (\theta,\theta_c)$ if $\theta < \mathrm{Re}\,\theta_c$ and (θ_c,θ) if $\theta > \mathrm{Re}\,\theta_c$. The integration contour in (5) encompasses all the poles of g_θ.

4 Asymptotic Analysis

The solution (5) may be decomposed as [3]

$$G(\mathbf{r},\mathbf{r}_c) = G^d + G^{\mathrm{GO}} + G^{\mathrm{trans}}, \quad (7)$$

G^d is the field diffracted by the tip, G^{GO} is the CGO field and G^{trans} represents a transitional field that provides a continuous transition across the geometrical boundaries [4]. In this work, we do not address the field in the transition zones and concentrate on the first two terms.

4.1 Tip Diffracted Field

As noted, we are mainly interested in the case where the beam hits near the tip, so that we have $\theta_c \simeq \theta_0 =$ real. Referring to the angular domain $\theta < 2\Theta - \pi - \theta_0$ which excludes the geometrically reflected field, the integration contour $\mathscr{C}$ in (5) can be deformed to the imaginary ν axis [8], so that G^d is given by (5) with g_θ replaced by g_θ^s of (6), and $\mathscr{C}$ replaced by an integral from $\nu = -1/2 - i\infty$ to $-1/2 + i\infty$.

The resulting expression for the tip diffraction may be further simplified for the case of a narrow cones, by expressing the Legendre functions involving Θ as power series of $\pi - \Theta$ [3]. For the soft boundary condition case in (6), the main contribution is due to the $\ell = 0$ term, and the resulting integral can be evaluated analytically, yielding the tip diffracted field [7, 8]

$$G^d(\mathbf{r},\mathbf{r}_c) \simeq \frac{e^{ikr_c}}{4\pi r_c}\frac{e^{ikr}}{r}\frac{-i}{2\pi k \ln\frac{1}{2}(\pi-\Theta)}\frac{1}{\cos\theta+\cos\theta_c}, \quad (8)$$

where the first term is the incident beam of (2) evaluated at the tip, the second term is a spherical wave emerging from the tip and the last term is the CS diffraction coefficient.

4.2 Complex Geometrical Optics Solution

A. Complex Rays

Following [9], a complex ray (CR) that emerges from a complex point $\mathbf{r}_c$ is defined by

$$\mathbf{r}(s) = \mathbf{r}_c + s\hat{\mathbf{s}} \quad (9)$$

$\hat{\mathbf{s}}$ is the CR direction such that $\hat{\mathbf{s}}\cdot\hat{\mathbf{s}} = 1$, and s is the *complex distance* along that CR. The propagation direction is defined by the direction of increasing $\mathrm{Re}\,s$.

B. Complex Extension of the Cone

CR tracing requires an analytic continuation of the cone surface into a complex space. This is done here by substituting the complex coordinates $x = x' + ix'', y = y' + iy'', z = z' + iz''$ into cone equation $x^2 + y^2 = z^2\ \tan^2(\pi - \Theta)$, with $\mathrm{Re}\,z < 0$.

C. The Direct Complex Rays

The CR from the complex source point $\mathbf{r}_c$ to any given real observation point $\mathbf{r}$ is found by calculating the distance $s(\mathbf{r},\mathbf{r}_c)$ of (2) with $\mathrm{Re}\,s(\mathbf{r},\mathbf{r}_c) > 0$, and then the corresponding ray direction $\hat{\mathbf{s}}$ via (9). In order to select the CR that are not blocked by the cone we . This calculate, using (9), the complex point $\mathbf{Q}$ where this CR (i.e., the one described by the $\hat{\mathbf{s}}$ found) intersects the cone surface. This also yields the distance $s(\mathbf{Q},\mathbf{r}_c)$ from $\mathbf{r}_c$ to $\mathbf{Q}$. Note that this procedure yields $s(\mathbf{Q},\mathbf{r}_c)$ uniquely and that $\mathrm{Re}\,s(\mathbf{Q},\mathbf{r}_c)$ may be positive or negative.

The direct ray selection rule: This ray is included in the field representation if $\mathbf{Q}$ does not belong to the complex extension of the cone (for example if $\mathrm{Re}\,z_Q > 0$), or if it does belong to the complex extension of the cone but has $\mathrm{Re}\,s(\mathbf{Q},\mathbf{r}_c) > \mathrm{Re}\,s(\mathbf{r},\mathbf{r}_c)$. Finally, if $\mathrm{Re}\,s(\mathbf{Q},\mathbf{r}_c) < 0$ then this ray is rejected.

The field of the resulting direct CR is given by G^i of (2).

D. Reflected Complex Rays

To find the reflected CR that reaches a real point $\mathbf{r}$, we first find the point $\mathbf{Q}$ where a given CR emerging from $\mathbf{r}_c$ intersects the complex extension of the scatterer, and then calculate $s(\mathbf{Q},\mathbf{r}_c)$. We also calculate $s(\mathbf{r},\mathbf{r}_c)$ where this ray intersects the real space at point $\mathbf{r}$. As noted above, this value is obtained uniquely via (9).

For each reflection point $\mathbf{Q}$ we then calculate the reflected CR direction $\hat{\mathbf{s}}^r$ by using the reflection law $\hat{\mathbf{s}}^r = \hat{\mathbf{s}}^i - (2\hat{\mathbf{s}}^i\cdot\hat{\mathbf{n}})\hat{\mathbf{n}}$ where $\hat{\mathbf{s}}^i$ is the direction of the incident ray and $\hat{\mathbf{n}}$ is normal to cone surface at $\mathbf{Q}$. Finally, we calculate the point $\mathbf{r}$ where this reflect CR intercepts the real space, and then calculate $s^r(\mathbf{r},\mathbf{Q})$, the complex distance from $\mathbf{Q}$ to $\mathbf{r}$.

The reflected ray selection rule: The ray is included in the reflected field representation only if $\mathbf{Q}$ belongs to the complex extension of the cone surface, and if $0 < \mathrm{Re}\,s(\mathbf{Q},\mathbf{r}_c) < \mathrm{Re}\,s(\mathbf{r},\mathbf{r}_c)$ and also $\mathrm{Re}\,s^r(\mathbf{r},\mathbf{Q}) > 0$.

The field of the reflected CR is given now by

$$u^r(\mathbf{r}) = G^i\Gamma\frac{e^{iks^r(\mathbf{r},\mathbf{Q})}}{\sqrt{J(\mathbf{r})}}, \quad (10)$$

where G^i is incident filed of (2), Γ is the reflection coefficient (here $\Gamma = -1$ for soft boundary) and J is the ray coor-

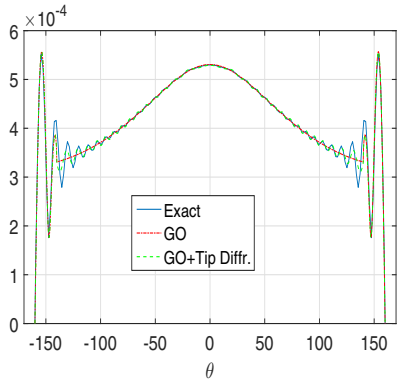

(a) Axial illumination: $\theta_0 = 0^\circ$

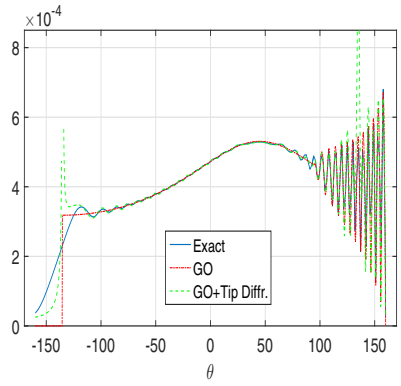

(b) Oblique illumination: $\theta_0 = 45^\circ$

Figure 2. The field due to a real point source. (a) source located on the z-axis at $(kr_0, \theta_0, \phi_0) = (50, 0^\circ, 0^\circ)$. (b) source at $(50, 45^\circ, 0^\circ)$. The figures compare the absolute value of the total field in the (x,z) plane calculated exactly via (3) (blue line), with the CGO field without and with the tip diffraction (solid-red and dashed-green lines, respectively). Negative θ correspond to points at $\phi = 180^\circ$.

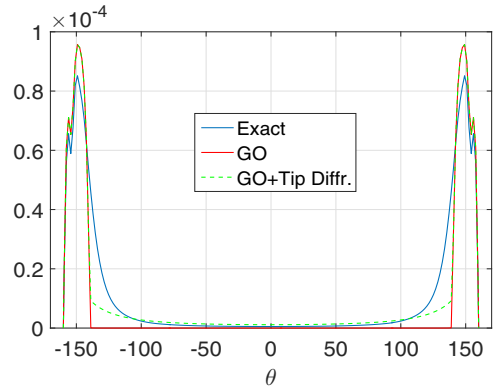

(a) Axial illumination on the tip

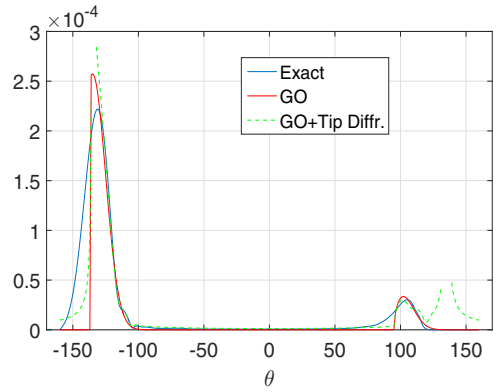

(b) Oblique illumination on the tip

Figure 3. As in Fig. 2, but for an incident CSB with $kb = 80$, hitting exactly at the tip. (a) axial illumination $k\mathbf{r}_0 = (kr_0, \theta_0, \phi_0) = (100, 0^\circ, 0^\circ)$ and $\hat{\mathbf{b}} = (\theta_b, \phi_b) = (180^\circ, 0^\circ)$. (b) oblique illumination $k\mathbf{r}_0 = (100, 45^\circ, 0^\circ)$ and $\hat{\mathbf{b}} = (135^\circ, 180^\circ)$.

dinates Jacobian that represents the geometrical ray spreading.

5 Numerical Examples

The goal in this section is to explore the asymptotic solutions vs. the exact solution for a cone with $\Theta = 160^\circ$. We present the total field as a function of the angle θ at the (x,z) plane at distance $kr = 200$ from the tip, calculated via the exact solution (3) (solid blue line), and the CGO solution (10) without and with the tip diffraction (8) (solid red and dashed-green lines, respectively).

To get insight and to validate the expression we consider first in Fig. 2 the field due to a real source located at a distance $kr_0 = 50$. We consider both axial illumination due to a source located on the z axis, or oblique illumination due to a source located at $\theta_0 = 45^\circ$. In Fig. 2(a), the GO plus diffraction provides a reasonable representation of the phenomenology even near the reflection boundary (RB) at $\theta = \pm 140^\circ$. In Fig. 2(b), the GO plus diffraction provides a reasonable representation of the phenomenology but the diffraction explodes at $\theta = \pm 135^\circ$ (see (8)). A transition function is needed for the transition zone.

Next, Fig. 3 depicts the field due to a collimated CSB with $kb = 80$, hitting exactly at the tip. Again we consider both axial and oblique illuminations. For the axial illumination, the waist is located at $k\mathbf{r}_0 = (kr_0, \theta_0, \phi_0) = (100, 0^\circ, 0^\circ)$ so that the beam direction is $\hat{\mathbf{b}} = (\theta_b, \phi_b) = (180^\circ, 0^\circ)$, giving the polar CS coordinates $(kr_c, \theta_c \phi_c) = (100 - i80, 0^\circ, 0^\circ)$. For the oblique illumination we choose $k\mathbf{r}_0 = (100, 45^\circ, 0^\circ)$, hence $\hat{\mathbf{b}} = (135^\circ, 180^\circ)$, giving $k\mathbf{r}_c = (100 - i80, 45^\circ, 0^\circ)$. As expected, in the beam case the scattered field is localized near the reflection and transmission boundaries. In Fig. 3(a), it is localized near $\theta = \pm 140^\circ$ whereas in Fig. 3(b), it is localized near $\theta = 95^\circ$ and $\theta = -135^\circ$. Again the GO plus diffraction provides a reasonable representation of the phenomenology, except for the transition zones where a transition function is needed. In Fig. 3(b), $\theta_c = 45^\circ = real$, hence the diffraction explodes at $\theta = \pm 135^\circ$ (see (8)).

Finally, Fig. 4 depicts the field due to the same obliquely incident CSB as in Fig. 3(b), but now its axis does not intercept the tip, but rather passes above or below the tip. Here we set $k\mathbf{r}_0 = (100, 45^\circ, 0^\circ)$ as in Fig. 3(b) but the beam axis is $\hat{\mathbf{b}} = (125^\circ, 180^\circ)$ or $\hat{\mathbf{b}} = (145^\circ, 180^\circ)$, respectively, giving $(kr_c, \theta_c \phi_c) = (99.41 - i79.26, 37.8^\circ + i4.5^\circ, 0^\circ)$ or $(99.41 - i79.26, 52.2^\circ - i4.5^\circ, 0^\circ)$, respectively. In Fig. 4(a), one

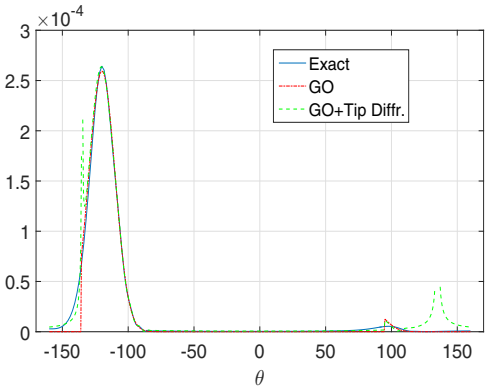

(a) Oblique illumination below the tip

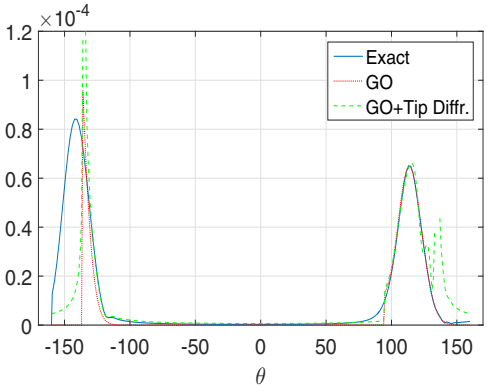

(b) Oblique illumination below the tip

Figure 4. As in Fig. 3(b), but for an obliquely incident CSB that hits off the tip. Here $k\mathbf{r}_0 = (100, 45^\circ, 0^\circ)$ as in Fig. 3(b) but in (a) the beam axis passes above the tip with $\hat{\mathbf{b}} = (125^\circ, 180^\circ)$, whereas in (b) the beam axis passes below the tip with $\hat{\mathbf{b}} = (145^\circ, 180^\circ)$.

readily observes a strong transmission around $\theta = -125^\circ$ and weak reflection around $\theta = 100^\circ$, whereas in Fig. 4(b), one observes a weak transmission and strong reflection. Furthermore, here θ_c is not real hence the diffraction does not explode at for any real θ (see (8)).

In summary, the asymptotic solutions provide a relatively good representation for all local phenomena, except for the geometrical reflection and shadow boundaries where a transition function is required.

6 Summary and Conclusions

We derived a new asymptotic solution for beam scattering by a hard or soft circular cone in terms of complex geometrical optics and complex-ray tip diffraction. This solution has been compared to an exact solution using complex spherical harmonics [2]. It is shown that the asymptotic solution describes the main phenomenology, except for the geometrical reflection and shadow boundaries where a transition function is required. As shown, the scattered beam field is localized in these transition zones, hence the derivation of such function is essential for the beam case. Such function has recently been derived for a wedge [11], and our long term goal is the derivation of such function for the cone. It is noted, though, that since the scattered beam field is localized, the spherical-harmonics solution may be used effectively as an alternative to such transition function.

7 Acknowledgements

EH acknowledges partial support by the Israeli Science Foundation (ISF), Grant No. 412/15.

References

[1] L.B. Felsen, "Complex-source-point solutions of the field equations and their relation to the propagation and scatering of Gaussian beams," in *Symposia Matematica, Istituto Nazionale di Alta Matematica*, Vol. **XVIII**, Academic Press, London, 1976, pp. 40–56.

[2] A. Reinhardt, H. Bruens, L. Klinkenbusch, M. Katsav and E. Heyman, "Spherical-multipole analysis of an arbitrarily directed complex-source beam diffracted by an acoustically soft or hard circular cone", *Adv. Radio Sci.*, vol. 13, pp. 57–61, 2015.

[3] L. Felsen, N. Marcuvitz, *Radiation and Scattering of waves*, Prentice-Hall, New Jersey, 1973.

[4] J. Bowman, B. A. Senior, P. L. E. Uslenghi, *Electromagnetic and Acoustic Scattering by Simple Shapes,* NH Amsterdam, 1969.

[5] E. Heyman and L.B. Felsen, "Gaussian beam and pulsed beam dynamics: Complex source and spectrum formulations within and beyond paraxial asymptotics," *J. Opt. Soc. Am. A*, vol. 18, pp. 1588–1611, July 2001.

[6] L.B. Felsen, "Alternative field representations in regions bounded by spheres, Cones, and Planes," *IRE Trans. Antennas Propagat.*, vol. 5, pp. 9–21, January, 1957.

[7] L.B. Felsen, "Asymptotic expansion of the diffracted wave for a semi-infinite cone", *IRE Trans. Antennas Propagat.*, vol. 5, pp. 403–404, October, 1957.

[8] L.B. Felsen, "Plane-wave scattering by small-angle cones", *IRE Trans. Antennas Propagat.*, vol. 5, pp. 122–129, January, 1957.

[9] Y.D. Wang and G.A. Deschamps, "Application of complex ray tracing to scattering problems," *Proceedings of the IEEE*, vol. 62(11), pp. 1541–1551, 1974.

[10] Y. Kravtsov, Y. Orlov, *Geometrical Optics of Inhomogeneous Media* , Springer, 1990.

[11] M. Katsav, and E. Heyman, "Converging and diverging beam diffraction by a wedge: A complex source formulation and alternative solutions," *IEEE Trans. Antennas Propagat.*, vol. 64, pp. 3080–3093, 2016.